Electric field measurements in atmospheric pressure discharges for plasma-assisted combustion and plasma flow control applications

I.V. Adamovich[1], M. Simeni Simeni[1], and Y. Tang[2]

[1]*Department of Mechanical and Aerospace Engineering, Ohio State University, Columbus, OH, USA*
[2]*Energy and Power Engineering, Tsinghua University, Beijing, China*

Abstract: Picosecond electric field induced second harmonic generation measurements have been done in ns pulse discharges in atmospheric pressure diffusion flames and in ambient air for several electrode geometries. The results demonstrate considerable potential of these techniques for electric field measurements in high-pressure plasmas, providing insight into kinetics of molecular energy transfer, plasma chemistry, energy thermalization rate, and coupling with the flow.

Keywords: second harmonic generation, ns pulse discharges, diffusion flame, electric field

1. Introduction

Measurements of electric field in weakly ionized plasmas in air, in fuel-air mixtures, and in flames are key to understanding the kinetics of chemical reactions among excited species and radicals produced in the plasma, their effect on the flow field, ignition, and flameholding [1,2]. In nonequilibrium plasmas, the electric field waveform controls the discharge input energy partition among internal energy modes of atoms and molecules, which determines the rates of production of excited species and radicals by electron impact, as well as the rates of plasma chemical reactions. This is critically important for low-temperature plasma-assisted fuel reforming, ignition, and combustion, driven by reactions of plasma-generated radicals species. In air flows, the rate of the discharge energy thermalization (sometimes referred to as "rapid heating") controls the localized thermal perturbations and the formation of large-scale coherent structures in the flow, which is the dominant effect in high-speed plasma flow control [1]. In flames, electric field also generates the body force on electrons and ions ("ion wind"), entraining the flow of neutral species and producing a strong effect on flame stability [3]. Detailed understanding of kinetics of these processes, as well as development of high-fidelity kinetic models of plasma flow control, plasma-assisted combustion, and flameholding requires electric field measurements using accurate, non-intrusive methods. This paper discusses recent progress in the use of Electric-Field Induced Second Harmonic (E-FISH) generation [4] for measurements of electric field in ns pulse dielectric barrier discharges used in surface plasma flow actuators and in laminar diffusion flames.

2. Experimental

The schematic of ps E-FISH experimental apparatus, shown in Fig. 1, is discussed in detail in our recent work [5-7]. Briefly, the fundamental output beam of an Ekspla PL2143A Nd:YAG laser, with a pulse duration of 30 ps and pulse energy of 2-10 mJ, operating at 10 Hz, is focused into the discharge / flame region, using a 100 cm focal distance lens. The signal beam is recollimated and focused onto the entrance slit of a monochromator, followed by a narrowband pass filter, and detected by a photomultiplier tube. The signal is proportional to the square of the electric field, averaged nearly uniformly over the span of the discharge electrodes. Individual electric field vector components are determined by isolating the second harmonic signals with different polarizations. Absolute calibration of the measurements is obtained from the known electrostatic electric field, calculated by solving the Laplace equation for a given electrode geometry.

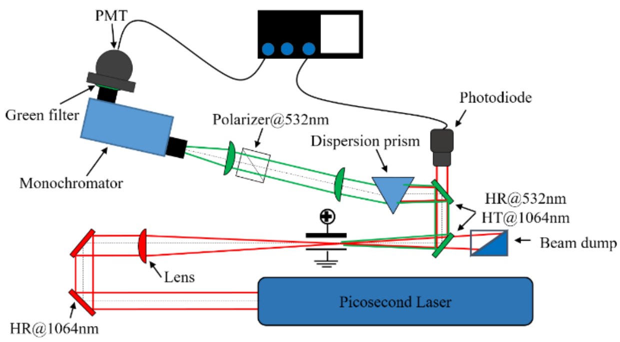

Fig. 1. Schematic of ps E-FISH generation apparatus.

Figure 2 shows a schematic of a high aspect ratio laminar diffusion flame burner (Burner 1) and the electrode assembly. The exit dimensions of the burner, made of quartz, are 0.5 mm x 45 mm. Hydrogen flows through the burner at the flow rate of 1-2 slm, maintaining

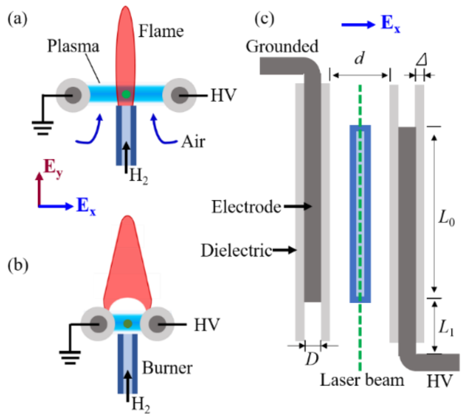

Fig. 2. Schematic of Burner 1.

a diffusion flame ≈ 50 mm long. Two parallel cylinder brass electrodes 3.2 mm in diameter, inside alumina ceramic tubes 6.4 mm in diameter, are placed slightly above the burner, separated by a gap of 4.5-15 mm. For large electrode gaps, 12-15 mm, the flame is attached to the burner, while for smaller gaps, 4-5 mm, it is attached to the top of the ceramic tubes, as shown in Fig. 2 (a,b). The laser beam is directed parallel to the electrodes.

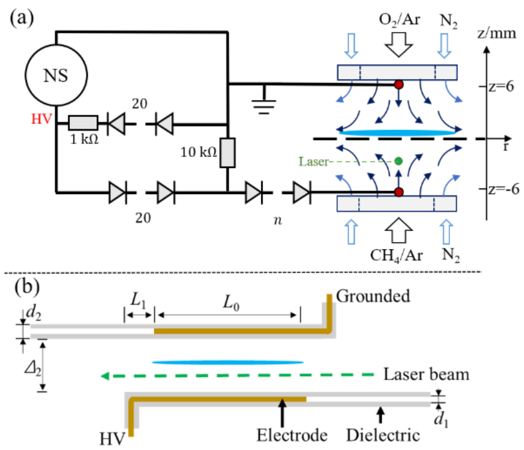

Fig. 3. Schematic of Burner 2.

Figure 3 shows a schematic of a counterflow burner (Burner 2) and electrode assembly. The burner sustains a laminar counterflow diffusion flame in a mixture of 14% CH_4-Ar (bottom) and 42% O_2-Ar (top), with the N_2 co-flow. The diameters of the inner and co-flow nozzles are 10 mm and 16 mm respectively, and the gap between the fuel and oxidizer nozzles is 15 mm. The flow rates of the fuel and oxidizer mixtures are 1.25 and 1.25 slm, and the co-flow rates are 2.25 slm (top) and 0.75 slm (bottom). The discharge is generated between two parallel brass rod electrodes 1.5 mm in diameter, covered by alumina ceramic tubes 3 mm in diameter, with the electrode gap of 12 mm.

Figure 4 shows a schematic of a ns pulse, surface dielectric barrier discharge plasma actuator. The actuator is made of an alumina ceramic plate 0.6 mm thick and two adhesive copper foil electrodes 25 mm wide and 100 µm thick, attached to the dielectric plate with no overlap.

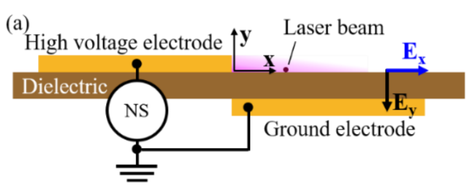

Fig. 4. Schematic of a surface plasma flow actuator.

In all three cases, the electrodes are powered by a high-voltage pulse generator producing alternating polarity pulses with peak voltage of up to 16 kV and pulse repetition rate of 20 Hz. The alternating polarity pulse train is converted to a positive or negative polarity 10 Hz pulse train by using high-voltage diodes connected in series between the pulse generator and the electrodes. In Burner 2, additional modification of the external circuit is used to add a gradually decaying tail to the voltage pulse shape, several ms long, without changing the pulse shape during the voltage rise. Discharge voltage and current are measured by Tektronix P-6015 high voltage probe and Pearson 2877 current probe. Plasma emission images are taken by Princeton Instruments PI-Max 3 ICCD camera with a UV lens.

3. Results and Discussion

Figure 5 plots the horizontal electric field in a positive polarity ns pulse, dielectric barrier discharge in a hydrogen-air flow below the flame in Burner 1 (see Fig. 2(a)). It can be seen that the electric field follows the applied voltage pulse until breakdown, when the current increases abruptly and the field decays rapidly due to the plasma self-shielding. The electric field reduction after the breakdown is consistent with the plasma emission images, which indicate the decay of the emission intensity between the electrodes, following breakdown. No detectable electric field offset is observed either before or after the discharge pulse, indicating that the residual surface charge accumulation from the previous pulse, as well the charge accumulation after the pulse, are insignificant at these conditions. The results show that during the discharge pulse, most of the energy is coupled to the hydrogen plasma at the electric fields of E ≈ 9-19 kV (reduced electric field of E/N ≈ 50-100 Td at the flow temperature of T=370 K, measured by N_2 CARS). At these conditions, over 50% of the input energy goes to H_2 electronic excitation and dissociation by electron impact, generating H atoms. However, no effect of the ns pulse discharge on the flame was detected at these conditions, due to the very slow mixing of the plasma-excited hydrogen flow with ambient air.

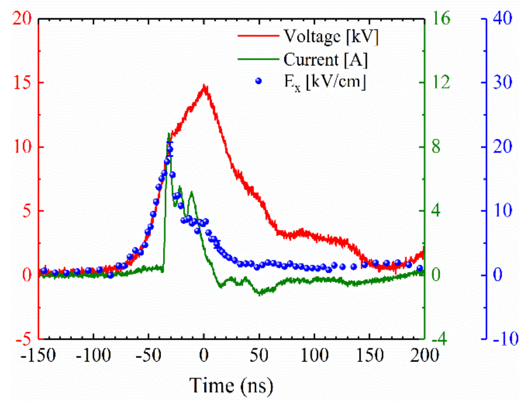

Fig. 5. Horizontal electric field in a ns pulse discharge in a hydrogen-air flow below the flame in Burner 1.

Figure 6 shows the results of the vertical electric field measurements in Burner 2, in a ns pulse discharge with a long tail (2 ms FWHM) at the trailing edge of the voltage pulse waveform. At these conditions, the deviation of the measured field from the Laplacian field is less pronounced than in Burner 1, suggesting that the electron density in the plasma is lower. It can also be seen that adding the tail generates a fairly significant electric field after the discharge pulse, in the range of 2-5 kV/cm at the measurement locations, on the time scale of several hundred ns. The electric field of approximately 1 kV/cm also persists during the entire period between the discharge pulses, 100 ms, due to the surface charge accumulation on the dielectric tubes covering the electrodes.

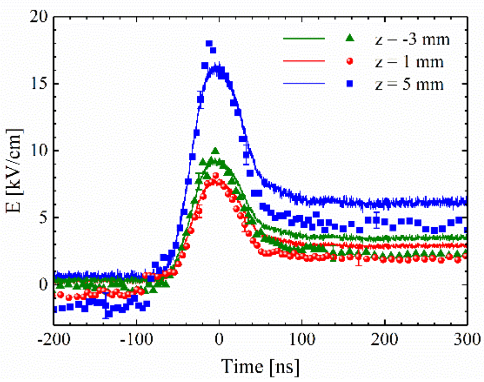

Fig. 6. Vertical electric field at different locations in Burner 2, during the ns discharge pulse with a 2 ms tail.

Figure 7 shows a set of flame emission images in a ns pulse discharge with a 6 ms long tail added to the voltage waveform. It can be seen that the flame exhibits high-amplitude oscillations, which are significantly stronger compared with those for the baseline case of pulses without the tail. Note that extending the voltage waveform tail does not change the pulse energy coupled to the plasma. Therefore at these conditions the effect on the flame is almost certainly due to the electrohydrodynamic interaction ("ion wind"). Since no additional ionization is generated during the voltage waveform tail, the enhanced effect of the flame is due to the transport of the ions produced during the discharge pulse by the electric field on a much longer time scale, enhancing the impulse of the body force.

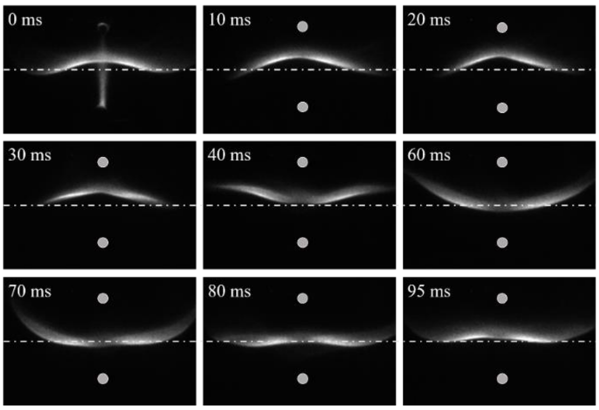

Fig. 7. Emission images illustrating flame oscillations excited by a ns pulse discharge with a 6 ms tail.

Figure 8 plots the horizontal and vertical electric field components in the surface plasma actuator (see Fig. 5), E_x and E_y, x=2 mm away from the high-voltage electrode and y≈100 μm from the dielectric surface, for the negative polarity pulse train. It can be seen that both E_x and E_y have a non-zero offset before the voltage pulse, due to the surface charge accumulation on the dielectric from the previous discharge pulse.

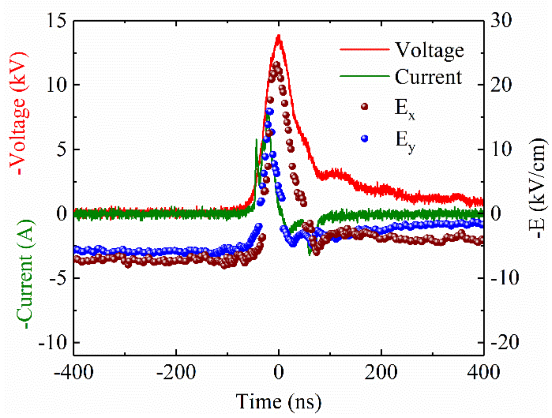

Fig. 8. Electric field components in the plasma actuator at x=2 mm, y≈100 μm, for the negative polarity pulse train.

During the potential increase on the high-voltage electrode, E_x and and E_y are first reduced to zero and then increase in the opposite direction. After breakdown, E_y drops rapidly, indicating the effect of plasma self-shielding. Peak electric field measured during the breakdown at this location is $E \approx 27$ kV/cm. The rise of the absolute value of E_x and and E_y during the voltage reduction indicates that they are inverted again and are now dominated by the field produced by the negative surface charge accumulated on the dielectric during the breakdown.

4. Summary

This work demonstrates a significant potential of ps E-FISH diagnostics for non-intrusive measurements of time-resolved and spatially-resolved electric field in atmospheric pressure plasmas and flames enhanced by ns pulse dielectric barrier discharges. The coherent second harmonic signal is easily separated from the fundamental laser beam, and discriminated against the plasma and flame emission.

In a low-temperature hydrogen-air plasma sustained below a hydrogen diffusion flame, the reduced electric field during the discharge pulse is E/N ≈ 50-100 Td, when over 50% of the input energy goes to H_2 electronic excitation and dissociation by electron impact, as expected. In a plasma-enhanced counterflow flame, combining ns pulses and ms time scale waveforms results in a strong effect of the plasma on the flame, due to the ionization produced by the ns pulses and the ion wind generated on the long time scale. These suggests that these waveforms may be used for plasma flame stabilization and flameholding.

In a ns pulse plasma actuator, the data show that surface charge accumulation strongly affects the electric field in the plasma (see Fig. 1). Also, the time scale for the electric field reduction in the plasma after breakdown is fairly long, several tens of ns, suggesting that a considerable fraction of the energy is coupled to the plasma at a relatively low reduced electric field, several tens of Townsend. This limits the discharge energy fraction thermalized as rapid heating, reducing the effect on the flow caused by the high-amplitude localized thermal perturbations.

In some cases, for relatively simple electrode geometries and in the absence of surface charge accumulation on dielectric surfaces, Laplacian electric field measured before breakdown may be used for absolute calibration (e.g. see Fig. 5), such that the technique becomes "self-calibrating". This is particularly important at the conditions when the mixture composition is not known, such as in plasma-enhanced flames and atmospheric pressure plasma jets. If such self-calibration does not apply, due to surface charge effects or ionization wave propagation, inference of the electric field in flames and plasma jets may be complicated considerably, by chemical reactions and mixing with ambient air species.

5. Acknowledgments

The support of US Department of Energy Center for Exascale Modeling of Plasma Assisted Combustion, US Department of Energy Plasma Science Center "Predictive Control of Plasma Kinetics: Multi-Phase and Bounded Systems" is gratefully acknowledged. We would also like to thank Dr. Benjamin Goldberg (Princeton University) for productive technical discussions.

6. References

[1] Y. Ju and W. Sun, Progress in Energy and Combustion Science, 48 (2015) 21

[2] S.B. Leonov, I.V. Adamovich, and V.R. Soloviev, Plasma Sources Science and Technology, 25 (2016) 063001

[3] D.A. Lacoste, Y. Xiong, J.P. Moeck, S.H. Chung, W.L. Roberts, and M.S. Cha, Proceedings of the Combustion Institute, 36 (2017) 4183

[4] A. Dogariu, B.M. Goldberg, S. O'Byrne, and R.B. Miles, Physical Review Applied, 7 (2017) 024024

[5] M. Simeni Simeni, Y. Tang, Y.-C. Hung, Z. Eckert, K. Frederickson, and I.V. Adamovich, Combustion and Flame, 197 (2018) 254

[6] M. Simeni Simeni, Y. Tang, K. Frederickson, and I.V. Adamovich, Plasma Sources Science and Technology, 27 (2018) 104001

[7] Y. Tang, M. Simeni Simeni, Q. Yao, K. Frederickson, and I.V. Adamovich, AIAA Paper 2019-0744, 2019 AIAA Aerospace Sciences Meeting (SciTech 2019), 7-11 January 2019, San Diego, CA